Encapsulation of food waste compounds in soy phosphatidylcholine liposomes: effect of freeze-drying, storage stability and functional aptitude

Marín, D., Alemán, A., Montero, P., and Gómez-Guillén, M.C.*

Institute of Food Science, Technology and Nutrition (ICTAN-CSIC). C/ José Antonio Novais 10, 28040 Madrid (Spain)

*Author for correspondence: mc.gomez@csic.es

Abstract

Liposomes made from soy phosphatidylcholine entrapping food waste compounds (collagen hydrolysate, L-HC; pomegranate peel extract, L-PG; and shrimp lipid extract, L-SL) were freeze-dried and stored for seven months. The freeze-drying process increased the particle size and decreased water solubility. The freeze-dried L-HC and L-PG preparations presented large multivesicular vesicles with spherical and unilamellar morphology. Large multilamellar vesicles were observed in L-SL, coinciding with greater structural changes in the membrane bilayer and increased thermal stability, as observed by ATR-FTIR and DSC. Dynamic oscillatory rheology revealed a slight hardening in the dried liposomes, induced by storage time. A sharp rigidifying effect in the temperature range from 40 to 90 °C was observed in L-SL. The loading with antioxidant compounds prevented freeze-drying-induced lipid oxidation. The storage stability of freeze-dried liposomes and their technological aptitude as a food ingredient varied depending on the chemical nature of the entrapped compounds.

Keywords: food; liposomes; soy phosphatidylcholine; lipid oxidation; freeze-drying; storage stability.

1. Introduction

Nowadays there is growing interest in the use of liposomes in the food industry in a variety of applications (Mozafari et al., 2008). Liposomes carrying bioactive compounds could be incorporated in functional foods for enrichment with healthy components or diseases prevention (Singh, 2016). Soy phosphatidylcholine-based liposomes have been used for encapsulating omega-3, omega-6, and vitamins E and C to fortify chocolate milk (Marsanasco et al., 2016) or orange juice (Marsanasco et al., 2015). The use of natural soybean lecithin for liposomal encapsulation in food applications provides nutritional value owing to its high essential polyunsaturated fatty acid profile with a beneficial role in lipid metabolism (Ramdath et al., 2017), and it does not raise any food legislation concerns (Laye et al., 2008). However, the predominantly highly unsaturated nature of soy lecithin could make this material very susceptible to lipid oxidation (Wang and Wang, 2008).

Liposomes are amphipathic spherical colloidal vesicles composed of one or more phospholipid bilayers around an aqueous core. This feature enables them to entrap and protect both hydrophilic and lipophilic bioactive materials, and to act as target delivery carriers in the organism (Mozafari et al., 2008). There is extensive recently published information on phosphatidylcholine liposomes loaded with a great variety of natural compounds with antioxidant properties, such as gelatin or collagen hydrolysates (Ramezanzade et al., 2017; Mosquera et al., 2014), polyphenolic compounds (Popova and Hincha, 2016; Lopes de Azambuja et al., 2015), or strong lipophilic compounds such as carotenoids (Du et al., 2015), tocopherol (Neunert et al., 2015) or essential polyunsaturated fatty acids (Semenova et al., 2016). However, differences in liposome composition and production procedure make it difficult to compare the physico-chemical properties of the resulting loaded vesicles.

Liposomes are normally presented in the form of aqueous liposomal suspensions, which could lose stability causing vesicle fusion or aggregation, leakage of the entrapped compounds and

sedimentation (Sharma and Sharma, 1997). Lyophilization is an alternative process for increasing the shelf life of liposomes, maintaining their stability by preserving them in a dry state (Stark et al., 2010). Drying liposomes is also a technological way of including vesicles in restructured fish products without negatively affecting their water content (Marín et al., 2018). However, freeze-drying may damage lipid bilayers by ice crystal formation during freezing, vesicle fusion/aggregation following dehydration and changes in phase transition during rehydration (Chen et al., 2010). Cryoprotectants, such as carbohydrates or polyalcohols, have been proposed to prevent freeze-drying-induced vesicle damage (Stark et al., 2010).

The aim of this work was to study the effect of freeze-drying and long-term storage on physico-chemical, structural, rheological and oxidative properties of glycerol-added liposomes entrapping various heat-sensitive food waste compounds with high added value, which could be used as functional food ingredients.

2. Materials and methods

2.1. Extraction of food waste compounds

Alcalase acid-soluble collagen hydrolysate (HC) was obtained from frozen squid (*Dosidicus gigas)* tunics following the procedure described in a previous work (Marín et al., 2018). The HC was spray-dried and stored at −20 °C until use. The HC hydrolysate was mostly composed of < 1.3 kDa peptide fractions (89 %), with major constituent amino acid residues of glycine, glutamic acid, alanine and aspartic acid (56 %), and total hydrophobic amino acids accounting for 28 % (Marín et al., 2018).

Pomegranate (*Punica granatum*) peel and albedo were dried in an oven at 50 °C overnight and grounded to obtain a fine powder, which was suspended in ethanol/water (70/30) at 1:20 (w/v) ratio and stirred at 40 °C for 4h. The mixture was left to stand at 21 °C overnight and

74 centrifuged at 12000g (at 4 °C for 15 min). The supernatant was filtered through Whatman
75 No.1 paper. The obtained extract (PG) was rotary-evaporated at 40 °C and stored at –20 °C
76 until use. The PG extract was mainly composed of ellagitannins (β-punicalagin, ellagic acid, and
77 α-punicalagin), being rutin and epigallocatechin also identified. The total phenolic content in
78 PG was 166 mg gallic acid eq./g dry extract (Marín et al., 2018).
79

80 The ethyl acetate-soluble lipid extract from shrimp (*L. vannamei*) waste (SL) was prepared and
81 characterized in a previous work (Gómez-Estaca et al., 2017). The SL extract was composed of
82 ≈80 % fatty acids, ≈13 % α-tocopherol, 6.5 % cholesterol and 0.7 % astaxanthin (free and
83 esterified). The PUFA proportion was 44 %. The SL was rotary-evaporated at 60 °C and stored
84 at –20 °C until use.
85

86 **2.2. Preparation of liposomes**

87 Partially purified phosphatidylcholine (PC) was obtained by dissolving soybean lecithin in ethyl
88 acetate (1:5, w/v) and subsequently performing five washes with acetone (Taladrid et al.,
89 2017). The PC powder was stored at –20 °C until use.

90 Liposomes L-HC, L-PG and L-SL were produced according to Marín et al. (2018). Each extract
91 (0.8 g) was dispersed in 80 mL of 0.2 M phosphate buffer (pH 7). Then PC (20 g) was added and
92 the dispersions were kept in a water bath at 80 °C for 1 h. Phosphate buffer (68 mL) and
93 glycerol (12 mL) were added, and the mixtures were kept at 80 °C for 1 h. The volume of the
94 suspension was completed with 240 mL of phosphate buffer. The samples were vortexed at 60
95 °C and sonicated in an ultrasonic cell disrupter (Model Q700, Qsonica sonicators, Newton, CT,
96 USA). The hydrodynamic particle stability of the newly prepared liposomal dispersions was
97 measured during two weeks at 4 °C. The freeze-drying process was performed by placing 50mL

of newly prepared liposomal dispersion in plastic cups of 100mL with perforated caps, which were frozen at -80 °C for 24h. Lyophilisation took place in a VirTis Freeze Drying Equipment (VirTis mod.6K TEL-85, coupled to TRIVAC-E2 pump) operating at a vacuum level of 0.13 mbar, with the collector starting at a temperature of −45 °C up to -80°C after 48h. All dried liposomes presented a pasty-like consistency rather than a fine powder appearance. The freeze-dried liposomes (liposomal pastes) were stored in darkness at –20 °C for seven months, in order to check their long-term storage stability.

2.3. Size, polydispersity and zeta potential

Particle size (z-average in intensity), polydispersity index (PDI) and zeta potential of fresh and rehydrated liposomes were measured using a Zetasizer Nano ZS (Malvern Instruments Ltd, Worcestershire, UK) in triplicate at 25 °C (Alemán et al., 2016). Freeze-dried liposomes were previously rehydrated by suspending in distilled water (77 mg/mL) at 20 °C for 30 min under magnetic stirring.

2.4. Entrapment efficiency

The entrapment efficiency (EE) was determined following the procedure of Marín et al. (2018), and calculated by the equation:

$$\% \text{ EE} = \text{encapsulated extract} / \text{total extract} * 100.$$

The encapsulated extract was calculated by difference between the total extract and the non-encapsulated extract. The non-encapsulated extract was quantified by: protein content with a LECO FP-2000 nitrogen/protein analyser for HC; phenolic content by the Folin–Ciocalteu method for PG; and astaxanthin content by spectrophotometric absorbance measurement at 470 nm for SL.

2.5. Moisture content and water solubility

Moisture was determined according to method 950.46 (A.O.A.C., 2005). Water solubility was determined after dilution in distilled water (1% w/v) at 20 °C for 150 min under magnetic stirring and centrifugation at 5000 g at 4 °C for 5 min. The supernatant was dried at 105 °C and the water solubility, expressed as a percentage, was calculated by weight difference with respect to the initial sample weight.

2.6. Cryo-transmission electron microscopy (cryo-TEM)

Cryo-TEM images of freeze-dried liposomes were obtained at –180 °C, using a JEOL JEM-1230 transmission electron microscope operating at 100 kV with a nominal magnification of 30K, as described previously (Taladrid et al., 2017).

2.7. Colour

The colour parameters, L* (lightness), a* (redness) and b* (yellowness) of freeze-dried liposomes, were measured using a Konica Minolta CM-3500d colorimeter (Konica Minolta, Madrid, Spain), with D65 illuminant and D10 standard observer. Hue angle and chroma values were calculated from L* a* b* values. Results were the average of 10 replicates.

2.8. Differential Scanning Calorimetry (DSC)

DSC analysis was performed using a model TA-Q1000 differential scanning calorimeter (DSC) (TA Instruments, New Castle, DE, USA) (Taladrid et al., 2017). All samples (≈10–12 mg) were scanned at a heating rate of 10 °C/min from –35 °C to 90 °C, under dry nitrogen purge (50 mL/min). Endothermic peak temperatures (T_{peak}, °C) and enthalpies of conformational changes (ΔH, J/g) were determined at least in triplicate.

145

146 **2.9. Attenuated Total Reflectance Infrared spectroscopy (ATR-FTIR)**

147 Infrared spectra of freeze-dried liposomes were recorded between 4000 and 650 cm^{-1} using a
148 Perkin Elmer Spectrum 400 Infrared Spectrometer (Perkin Elmer Inc., Waltham, MA, USA)
149 equipped with an ATR prism crystal accessory as described previously (Taladrid et al., 2017).

150

151 **2.10. Dynamic oscillatory rheology**

152 Viscoelastic properties (G', G", δ) of freeze-dried liposomes were determined in a Bohlin
153 rheometer (Bohlin Instruments Ltd., model CVO-100, Worcestershire, UK), using a cone-plate
154 geometry (cone angle 4°, gap 0.15 mm). A dynamic frequency sweep was performed by
155 applying oscillation amplitude at 5% strain over the frequency range 0.1–10 Hz at 10 °C. The
156 mechanical spectra with the elastic modulus (G'; Pa) and viscous modulus (G"; Pa) were
157 plotted as functions of frequency. To characterize the frequency dependence of G' over the
158 limited frequency range, the power law was used:

159 $$G' = G_0'\omega^{n'}$$

160 where G_0' is the energy stored and recovered per cycle of sinusoidal shear deformation at a
161 frequency of 1 Hz, ω is the frequency and *n'* is the power law exponent, which should exhibit
162 an ideal elastic behaviour near zero. A temperature sweep test was performed by heating from
163 20 to 90 °C at 1 °C/min and frequency of 1 Hz. Values of G' and G" were plotted as functions of
164 temperature. At least two determinations were performed for each sample. The experimental
165 error was lower than 6% in all cases.

166

167 **2.11. Lipid oxidation**

Lipid oxidation was measured by the thiobarbituric acid reactive substances (TBARS) method. Liposomes were mixed with 7.5% trichloroacetic acid solution (1:3 w/v) and centrifuged at 5100 g for 5 min at 4 °C. Then 0.02 M thiobarbituric acid was added to the supernatant (2:1 v/v) and kept at 20 °C for 15 hours in darkness. Absorbance was measured at 532 nm. Results were expressed as µg of malondialdehyde (MDA) equivalent per kg of sample, based on a 1,1,3,3-tetraethoxypropane (TEP) standard curve. Samples were analysed at least in triplicate.

2.12. Statistical analyses

Analysis of variance was performed using the SPSS® computer program (IBM SPSS Statistics 22 Software, Inc., Chicago, IL, USA). Differences among samples were established using the Tukey test, with a significance level set at $p \leq 0.05$.

3. Results and discussion

3.1. Particle characterization

The three freshly loaded liposomes did not differ ($p > 0.05$) in particle size, polydispersity index and zeta potential (Table 1). The empty liposomes (L-E) presented lower ($p \leq 0.05$) z-average and zeta potential than the loaded liposomes. The PDI, which reflects particle size distribution, oscillated between 0.24 and 0.26; the PDI is considered a good index when it is below 0.3. The strong electronegative zeta potential values were indicative of the high stability of all the liposomal suspensions (Müller et al., 2001). The loading with HC, PG or SL contributed slightly to an increase in the surface membrane charge, providing increased stability to the respective liposomal suspensions.

190 Fresh liposomes stored at 4 °C for 2 weeks showed no significant changes in size and PDI, while
191 the zeta potential experienced only a very slight decrease ($p \leq 0.05$) in L-HC and L-SL at the end
192 of the second week of storage (Table 1). These results confirmed the high stability of the fresh
193 liposomal suspensions during short-term storage.

194 The freeze-drying process caused increases ($p \leq 0.05$) in the liposome z-average and zeta
195 potential (Table 1). The changes in PDI were more accentuated in L-SL, which changed from
196 0.246 to 0.408. An increase in size and polydispersity when a small liposome is freeze-dried has
197 been reported previously and attributed to fusion or aggregation phenomena during water
198 removal (Chen et al., 2010) and to swelling of the bilayer upon rehydration (Stark et al., 2010).

199 To check the storage stability of the freeze-dried liposomes, their particle properties after
200 rehydration were characterized at 0, 3 and 7 months (Table 1). Immediately after freeze-
201 drying, L-SL had the largest size and polydispersity. The zeta potential was similar in all
202 formulations and showed a slight tendency to decrease ($p \leq 0.05$) with time. The liposomes with
203 the entrapped compounds showed a decrease ($p \leq 0.05$) in z-average at month 3, while the
204 empty liposome showed a more gradual size reduction from months 0 to 7. The PDI of L-SL
205 changed considerably from 0.408 to 0.258 at month 7, coinciding with the most pronounced
206 decrease in z-average.

207

208 **3.2. Moisture and water solubility**

209 The moisture content decreased in all the dried liposomes without significant differences
210 depending on the entrapped compound (Table 2). Ye et al. (2017) reported a water content
211 <15% for all their freeze-dried liposomes. The higher hydration level observed in the present
212 work could be attributed to the use of glycerol for liposome production, in agreement with
213 Manca et al. (2013). The highly hygroscopic nature of glycerol inhibited the formation of a dry

lyophilized powder, providing samples with a gluey and pasty texture, as reported previously (Taladrid et al., 2017). Unlike the empty liposome, moisture content was significantly ($p \leq 0.05$) reduced in the freeze-dried liposomes loaded with the various natural compounds within the first 3 months of storage and thereafter. The rearrangement of residual water molecules in the first stages of frozen storage could cause destabilization of water interactions with glycerol in the presence of the entrapped compounds, probably favouring water evaporation during moisture content determination. This finding provides first indication that the entrapped compounds could cause structural changes in the liposomal membrane.

The fresh L-E suspension had a water solubility significantly lower ($p \leq 0.05$) than in L-HC, L-PG and L-SL (Table 2). This difference might reflect structural changes in the membrane bilayer resulting from interactions with the entrapped compounds that led to a decrease in vesicle aggregation. When the liposomes were freeze-dried, a pronounced decrease in water solubility was found in L-SL, indicating higher vesicle aggregation.

3.3. Entrapment efficiency

Immediately after freeze-drying, the entrapment efficiency for L-HC, L-PG and L-SL was, respectively, 87%, 63% and 97% (Table 3). The EE in all the formulations remained stable ($p > 0.05$) during 7 months of storage, in agreement with Laverman et al. (2000) for freeze-dried liposomes stored for one year.

The higher entrapment in L-SL was attributed to the lipid nature of the shrimp extract, which enabled greater allocation within the fatty acid acyl chains of the membrane bilayer. Because of the poor water solubility of SL, it was more difficult for it to leak out from the liposomes upon rehydration (Chen et al., 2010). In the liposomes loaded with HC and PG, their hydrophilic components would be mostly entrapped in the inner aqueous core of the

liposome. In the case of L-PG, the lower EE would indicate that a considerable amount of phenolic compounds remained outside the vesicles. Subsequent changes in membrane fluidity during the storage period could be responsible for the size reduction in all the preparations, but they did not cause leakage of the entrapped compounds.

3.4. Colour

Freeze-dried L-E and L-HC samples showed higher ($p \leq 0.05$) values of luminosity (L*) and yellowness (b*) than L-PG and L-SL (Table 4). Parameter a* (redness) was highest for L-SL. Encapsulation of the collagen hydrolysate caused very slight changes in liposome coloration, the appearance changing from yellowish in L-E to light brown in L-HC. The pomegranate extract caused notable darkening in L-PG, probably due to the remaining non-encapsulated extract in this sample. The noticeable orange colour in L-SL (hue angle of 39°) was attributed to the carotenoid content in the shrimp lipid extract (Gómez-Estaca et al., 2017). According to Hama et al. (2012), the preferential location of the astaxanthin terminal rings on the liposomal membrane surface could be mainly responsible for the orange colour of the L-SL sample. The colour parameters of the various freeze-dried liposomes did not change during the storage time (data not shown).

3.5. Cryo-transmission electron microscopy

The cryo-TEM images of fresh liposomes showed similar morphology and particle size distribution for empty and loaded liposomes, most of them being spherical, well-separated unilamellar vesicles, although a few liposomes showed a bivesicular configuration (Figure 1). The vesicles had different sizes, according to the polydispersity shown in Table 1, with a greater abundance of small vesicles than of large ones. The freeze-dried L-HC and L-PG

liposomes showed large multivesicular vesicles, more pronouncedly in L-PG, without losing their characteristic spherical and unilamellar morphology (Figure 2). In the L-SL paste, large multilamellar vesicles and also morphologies with a varying degree of invagination were observed.

3.6. Differential scanning calorimetry

DSC results of fresh liposomal suspensions and freeze-dried pastes are presented in Figure 3 and Table 5. Liposome suspensions were characterised by a highly cooperative endothermic transition at sub-zero temperatures (T_{peak1}). L-HC, L-PG and L-SL exhibited a slight increase ($p \leq 0.05$) in T_{peak1} as compared to the empty liposomes. The inclusion of the extracts increased ($p \leq 0.05$) the enthalpy (ΔH) by around 39–43% with respect to the empty liposomes, in agreement with previous work on asolectin-genistein liposomes (Lopes de Azambuja et al., 2015). Fresh empty liposomes (L-E) showed a second minor endothermic event (T_{peak2}) at 10.8 °C (ΔH = 2.97 J/g), which was not observed in the other liposomal preparations within the range of temperatures tested (–30 to 90 °C). These findings indicated structural changes in the membrane bilayer, probably owing to interactions of the entrapped compounds with the polar head groups and their intercalation in the bilayer membrane.

The DSC traces of the freeze-dried pastes showed more diffuse endothermic transitions as a result of the reduced moisture content (Figure 3b, Table 5). The main transition shifted to 4 °C in L-E, 2 °C in L-HC and L-PG, and 11 °C in L-SL, with very weak enthalpy values (data not shown). The increase in the main Tm of the lipid membrane upon lyophilisation was ascribed to decreased head group spacing causing large compressive stress in the lipids in the dry state (Koster, Lei, Anderson, Martin & Bryant, 2000). The higher T_{peak} in the dried form of L-SL would indicate that the predominant liposoluble compounds in the shrimp extract (namely fatty acids, tocopherol, astaxanthin and cholesterol) were strongly embedded inside the lipid

bilayer, contributing to an increase in the stability of the liposomal membrane. In particular, cholesterol has been widely reported as an active agent providing rigidity and stability to phosphatidylcholine bilayer membranes (Sułkowski et al., 2005). The presence of large multilamellar vesicles in L-SL after freeze-drying would also contribute to an increase in the thermal stability. The transition temperature in L-E showed a progressive decrease during the storage period. A significant decrease ($p \leq 0.05$) was also found in L-HC after seven months of storage. In contrast, T_{peak} of L-PG and L-SL pastes remained unchanged ($p > 0.05$) during the whole storage period.

3.7. Infrared spectroscopy (ATR-FTIR)

Infrared spectroscopy was used to evaluate structural and conformational changes caused by entrapment of the various compounds at different parts of the bilayer (Toyran et al., 2003). Figure 4 depicts changes in frequency peaks immediately after freeze-drying and after 3 and 7 months of frozen storage.

Variations in wavenumbers at ≈2925 cm^{-1} and ≈2850 cm^{-1}, related respectively to CH_2 asymmetric and symmetric stretching vibrations, revealed changes occurring in the bilayer acyl chains. The downshift in the 2925 cm^{-1} band in newly freeze-dried liposomes was only observed in L-SL, indicative of greater stiffness in the deep interior of the bilayer (Figure 4a). The lipophilic nature of the SL caused an ordering effect through hydrophobic interactions with the membrane acyl chains, in agreement with reported work on liposomes loaded with different hydrophobic compounds (Toyran et al., 2003; Lopes de Azambuja et al., 2015; Pawlikowska-Pawlęga et al., 2014). This finding was in agreement with the higher thermal transition temperature observed by DSC. The apparent lack of intercalation into the aliphatic chain zone of the phenolic PG extract in the present study could be due to its lower hydrophobic nature in comparison with pure flavonoids used in other works, and also to the

312 relatively low entrapment efficiency. The storage period shifted the peak frequency at ≈2925
313 cm^{-1} towards lower values in all the liposomes, indicating an increase in membrane rigidity,
314 which coincided with the particle size reduction in all the freeze-dried liposomes during
315 storage.

316 Slight variations were observed in the C=O stretching absorption band at ≈1740 cm^{-1} (Figure
317 4b), related to structural changes associated with the hydration state of carbonyl groups at the
318 interfacial part of the membrane (Toyran et al., 2003). Loading with the various extracts hardly
319 altered the peak frequency with respect to the empty liposomes, indicating little interaction of
320 the loaded compounds with the ester carbonyl groups. The decrease in peak frequency at
321 ≈1740 cm^{-1} during storage in L-SL and L-PG might indicate variable interactions of the loaded
322 compounds at this membrane level. However, the downshift also observed in L-E at month 7
323 suggested that the dehydration of carbonyl groups could also be a result of intrinsic structural
324 changes in the membrane.

325 The PO_2^- antisymmetric double bond stretching at ≈1220 cm^{-1} revealed information related to
326 the phospholipid polar head groups of the membrane (Figure 4c). The upwards shift observed
327 in all the loaded liposomes as compared to the empty ones indicated a noticeable reduction in
328 the hydration state of the phosphate groups as a result of strong hydrogen bonding with the
329 various extracts, in descending order, L-SL, L-PG and L-HC. A similar FTIR event was reported in
330 liposomes loaded with genistein (Lopes de Azambuja et al., 2015). The stronger dehydration at
331 the membrane surface observed in the L-SL preparation coincided with higher vesicle
332 aggregation resulting from freeze-drying (lower water solubility). After 3 months of storage of
333 L-E and L-HC, and 7 months in the case of L-PG, a considerable increase in the peak frequency
334 at ≈1220 cm^{-1} was observed, which did not occur in L-SL. The greater stiffness in the deep
335 interior of the bilayer and strong hydrogen bonding with polar head groups in L-SL probably
336 restricted conformational changes in the course of time.

337

338 **3.8. Rheological properties**

339 The mechanical spectra representing the frequency dependence of the elastic (G') and viscous
340 (G") moduli immediately after freeze-drying are shown in Figure 5. All spectra fitted the power
341 law model (R^2 > 0.99), presented slightly higher values of G" than G', and phase angle >45°.
342 These results indicated that the dried liposomal pastes presented viscoelastic behaviour typical
343 of a highly viscous fluid rather than a solid material, attributed to the plasticizing effect of
344 glycerol. This property makes them suitable to be incorporated as functional ingredients in
345 restructured meat or fish products. The viscoelastic parameters of the freeze-dried pastes at 1
346 Hz and the value of the exponent n', obtained from fitting the mechanical spectra of G' to the
347 power law equation are presented in Figure 6. The entrapment with the various extracts led to
348 an increase in both G' and G", without noticeable changes in the phase angle. These results
349 indicate that the loaded freeze-dried liposomes became harder without substantially changing
350 their viscoelastic nature. This effect was attributed to interactions of the entrapped
351 compounds with the membrane polar head groups. The structural stability of the liposomal
352 pastes was determined from the value of the power law exponent (n'): the higher the n'
353 values, the higher the instability of the matrix against frequency changes. The n' was highest
354 ($p \leq 0.5$) in L-PG, indicating greater matrix discontinuity. The viscous modulus (G") in L-PG was
355 much greater than in the other preparations. These effects could be due to the lower
356 entrapment efficiency determined in L-PG, in which the non-encapsulated compounds would
357 have slightly hindered interactions among the dried lipid vesicles. This finding agrees with the
358 higher water solubility of this sample immediately after freeze-drying (Table 2).

359 After 7 months of storage, all samples, except L-PG, showed noticeably higher G' and G"
360 values, L-E being the preparation that registered the most pronounced increase. These results
361 indicate that the liposomal pastes tended to harden during the storage period, in agreement

362 with the increase in membrane rigidity as observed by FTIR. Changes in phase angle and in n'
363 were rather low, so the viscoelastic nature of the liposomal pastes did not change substantially
364 with storage time. In the case of L-PG the sample hardening was not clearly evidenced, but the
365 slight reduction of phase angle and n' suggested a slight increase in matrix stability.

366 All preparations presented a decreasing tendency in G' and G" with the rise in temperature,
367 with the exception of L-SL (Figure 7). This loss of consistency could be due to the heat-induced
368 disruption of interactions responsible for adhesion forces between adjacent lipid bilayers and
369 also between lipids within the bilayer (Augustyńska et al., 2016). Temperature plays a key role
370 in modifying local lipid orientation and producing a less ordered lipid arrangement, with the
371 result that inner interactions would be weakened. Tan et al. (2013) reported a heat-induced
372 decrease in the microviscosity of egg yolk phosphatidylcholine liposomes associated with a
373 decrease in membrane fluidity when the temperature increased above 50 °C.

374 The L-SL sample showed a pronounced increase in G' from 40 °C to 90 °C, indicating the
375 formation of a strong heat-induced gel-like structure. The SL extract stabilized the membrane
376 mechanical strength and favoured resistance to rupture at high temperatures. Similar findings
377 were obtained by Augustyńska et al. (2016) for liposomes encapsulating β-carotene. Tan et al.
378 (2013) demonstrated that the incorporation of lutein enhanced membrane rigidity by
379 restricting the motion freedom of lipids through interactions with lutein molecules. In
380 particular, hydrophobic interactions were reported to be the main reason for the structural
381 stability of the lipid bilayer upon heating up to 80 °C. In the present work, the sharp heat-
382 induced rigidifying effect observed when heating above 40 °C in L-SL suggested a
383 predominance of thermostable hydrophobic interactions occurring at high temperatures. The
384 thermal behaviour of the various liposomal preparations remained practically the same during
385 long-term storage, but registering higher values of G' and G" from the onset of heating. This
386 effect was probably the result of increased adhesion forces between lipid vesicles and also an

increase in membrane stiffness with time. However, the mainly responsible interactions kept their susceptibility to heat-induced breakdown. In the case of L-SL above 40 °C, the hydrophobic heat-induced interactions still helped to form an even stronger gel-like structure, as compared to that obtained immediately after-freeze-drying.

3.9. Lipid oxidation

The phosphatidylcholine (PC) used in this work is highly unsaturated, with linoleic acid accounting for ≈59% of the total fatty acids (Taladrid et al., 2017). The predominance of polyunsaturated fatty acids may generate hydroperoxides and secondary oxidation products leading to the accumulation of TBARS in soy lecithin emulsions (Wang and Wang, 2008). The MDA equivalent content in all the liposomal preparations is shown in Table 2. For the fresh liposomal suspensions, all TBARS were very low (8.22–18.4 μg/kg, expressed on a dry basis). The MDA equivalent content determined in the raw phosphatidylcholine (22.63 ± 0.86 μg/kg) was slightly higher than in the fresh liposomes, probably because the formation of the lipid bilayer limited the interaction of the reactive substances with the TBA. Therefore, no perceptible accumulation of secondary products of lipid oxidation could be attributed to the liposome preparation procedure. It should be noted that the PC used for liposome production presented significant residual amounts of tocopherol species, including α-tocopherol (Taladrid et al., 2017), which is a well-recognized antioxidant.

The TBARS increased ($p \leq 0.05$) in all freeze-dried liposomes probably favoured by structural and conformational changes in the bilayer that might have increased the exposure of hydrophobic compartments to the environment. Oxygen and free radicals are more soluble in the fluid lipid bilayer than in the aqueous solution. In particular, the presence of dihydrogen phosphate ions in the phosphate buffer solution was reported to decrease oxygen solubility and associated liposome oxidation (Guner & Oztop, 2017). Thus, oxygen concentration in the

412 interior organic phase of the membrane upon dehydration would have probably promoted
413 lipid oxidation (Pamplona, 2008).

414 At this time, L-PG was the liposome with the lowest MDA equivalent content, while L-E had the
415 highest one. The higher MDA equivalent content in L-E suggested that the loading with
416 antioxidant compounds could prevent some lipid oxidation after freeze-drying. The inhibition
417 of lipid peroxidation might be a consequence of the combination of two mechanisms: (1) the
418 intrinsic antioxidant property of the added compounds, and (2) their effects on the membrane
419 properties by limiting molecular oxygen penetration into the lipid bilayer (Tan et al., 2013). The
420 extracts used in the present study have been reported to have antioxidant capacity, which is
421 normally higher in the case of phenolic compounds, carotenoids and tocopherol than in
422 collagen hydrolysates (Alemán et al., 2011; Gómez-Estaca et al., 2017; Masci et al., 2016).
423 Probably for this reason, the prevention of freeze-drying-induced TBARS accumulation was
424 significantly lower in L-HC as compared to L-PG or L-SL. During the 7 months of storage the
425 TBARS value gradually decreased ($p \leq 0.05$) in all cases, with L-SL having the lowest values at the
426 end of the storage time. The unexpected reduction in TBARS values could be indicative of lipid
427 oxidative instability. A great diversity of phospholipid oxidation products and aldehydes are
428 generated during lipid peroxidation of polyunsaturated fatty acids (Catalá, 2009). Some of
429 them are very reactive and unstable molecules, so that their presumptive interaction with
430 liposome phospholipids would explain the decline in measured TBARS. Signs of lipid oxidation
431 in freeze-dried empty liposomes during the storage time, observed by FTIR, are shown in
432 Figure 8. The progressive decrease in the intensity absorbance in the region between 3600 and
433 3100 cm^{-1} with the concomitant increase and broadening of the band at ≈1740 cm^{-1}, would be
434 indicative of progressive decomposition of hydroperoxides to yield aldehydes and ketones. The
435 band at ≈1740 cm^{-1} was already proposed as useful infrared marker of the formation of
436 secondary lipid oxidation products in liposomes (Lamba et al., 1991). Similar behaviour was
437 found in freeze-dried liposomes entrapping the various compounds (data not shown),

indicating that lipid oxidation was not efficiently prevented during storage, even at frozen conditions.

3.10. Conclusions

The freeze-drying process caused structural changes in the membrane bilayer depending on the chemical nature of the entrapped compounds and their encapsulation efficiency. The loading with the various extracts did not negatively affect the mechanical stability of the freeze-dried liposomes during storage and prevented lipid oxidation. Liposomes loaded with lipophilic compounds may suffer a strong heat-induced rigidifying effect which should be considered in thermally treated foods. Dry liposomes entrapping bioactive compounds could serve as potential ingredients with long-term storage stability for designing functional food products with low or intermediate moisture level. To avoid oxidative instability of freeze-dried liposomes, various strategies could be proposed, such as optimization of the freeze-drying procedure or further membrane stabilization with amphiphilic antioxidants.

Acknowledgements

The authors wish to thank the Spanish MINECO for financial support (project AGL2014-52825). We are grateful to the Analysis Service Unit of ICTAN-CSIC for the DSC analysis, and to the Electron Microscopy Facility (EMF) at CIB-CSIC for the CryoTEM analysis.

References

Alemán, A., Giménez, B., Pérez-Santín, E., Gómez-Guillén, M.C, Montero, P. (2011). Contribution of Leu and Hyp residues to antioxidant and ACE-inhibitory activities of peptide sequences isolated from squid gelatin hydrolysate. *Food Chemistry*, 125, 334–341.

Alemán, A., Mastrogiacomo, I., López-Caballero, M.E., Ferrari, B., Montero, P. Gómez-Guillén, M.C. (2016). A novel functional wrapping design by complexation of ε-polylysine with liposomes entrapping bioactive peptides. *Food and Bioprocess Technology*, 9, 1113–1124.

A.O.A.C. (2005). Official methods of analysis. Gaithersburg, MD, USA: Association of Official Analytical Chemists.

Augustyńska, D., Burda, K., Jemioła-Rzemińska, M., Strzałka, K. (2016). Temperature-dependent bifurcation of cooperative interactions in pure and enriched in β-carotene DPPC liposomes. *Chemico-Biological Interactions*, 256, 236–248.

Catalá, A. (2009). Lipid peroxidation of membrane phospholipids generates hydroxy-alkenals and oxidized phospholipids active in physiological and/or pathological conditions. *Chemistry and Physics of Lipids*, 157, 1-11.

Chen, C., Han, D., Cai, C., Tang, X. (2010). An overview of liposome lyophilization and its future potential. *Journal of Controlled Release*, 142, 299–311.

Du, H.-H., Liang, R., Han, R.-M., Zhang, J.-P., Skibsted, L.H. (2015). Astaxanthin Protecting Membrane Integrity against Photosensitized Oxidation through Synergism with Other Carotenoids. *Journal of Agricultural and Food Chemistry*, 63, 9124–9130.

Gómez-Estaca, J., Calvo, M.M., Álvarez-Acero, I., Montero, P., Gómez-Guillén, M.C. (2017). Characterization and storage stability of astaxanthin esters, fatty acid profile and α-tocopherol of lipid extract from shrimp (L. vannamei) waste with potential applications as food ingredient. *Food Chemistry*, 216, 37–44.

Guner, S., Oztop, M.H. (2017). Food grade liposome systems: Effect of solvent, homogenization types and storage conditions on oxidative and physical stability. Colloids and Surfaces A: Physicochemical and Engineering Aspects, 513, 468-478.

Hama, S., Uenishi, S., Yamada, A., Ohgita, T., Tsuchiya, H., Yamashita, E., Kogure, K. (2012). Scavenging of hydroxyl radicals in aqueous solution by astaxanthin encapsulated in liposomes. *Biological and Pharmaceutical Bulletin*, 35 (12), 2238–2242.

Koster, K.L., Lei, Y.P., Anderson, M., Martin, S., Bryant, G. (2000). Effects of vitrified and nonvitrified sugars on phosphatidylcholine fluid-to-gel phase transitions. *Biophysical Journal*, 78, 1932–1946.

Lamba, O.P., Lal, S., Cecilia Yappert, M., Lou, M.F., Borchman, D. (1991). Spectroscopic detection of lipid peroxidation products and structural changes in a sphingomyelin model system. *Biochimica et Biophysica Acta (BBA)/Lipids and Lipid Metabolism*, 1081, 181-187.

Laverman, P., Van Bloois, L., Boerman, O.C., Oyen, W.J.G., Corstens, F.H.M., Storm, G. (2000). Lyophilization of Tc-99m-HYNIC labeled PEG-liposomes. *Journal of Liposome Research*, 10 (2–3), 117–129.

Laye, C., McClements, D.J., Weiss, J. (2008). Formation of biopolymer-coated liposomes by electrostatic deposition of chitosan. *Journal of Food Science*, 73 (5), N7–N15.

Lopes de Azambuja, C.R., Gomes dos Santos, L., Rodrigues, M.R., Rodrigues, R.F.M., Ferreira da Silveira, E., Azambuja, J.H., Flores, A.F.C., Horn, A.P., Dora, C.L., Muccillo-Baisch, A.L.,

Manca, M.L., Zaru, M., Manconi, M., Lai, F., Valenti, D., Sinico, C., Fadda, A.M. (2013). Glycerosomes: A new tool for effective dermal and transdermal drug delivery. International *Journal of Pharmaceutics*, 455, 66–74.

504 Marín, D., Alemán, A., Sánchez-Faure, A., Montero, P., Gómez-Guillén, M.C. (2018). Freeze-
505 dried phosphatidylcholine liposomes encapsulating various antioxidant extracts from natural
506 waste as functional ingredients in surimi gels. Food Chemistry, 245, 525-535.

507 Marsanasco, M., Calabró, V., Piotrkowski, B., Chiaramoni, N.S., del V. Alonso, S. (2016).
508 Fortification of chocolate milk with omega-3, omega-6, and vitamins E and C by using
509 liposomes. *European Journal of Lipid Science and Technology*, 118, 1271–1281.

510 Marsanasco, M., Piotrkowski, B., Calabró, V., del Valle Alonso, S., Chiaramoni, N.S. (2015).
511 Bioactive constituents in liposomes incorporated in orange juice as new functional food:
512 thermal stability, rheological and organoleptic properties. *Journal of Food Science and*
513 *Technology*, 52, 7828–7838.

514 Masci, A., Coccia, A., Lendaro, E., Mosca, L., Paolicelli, P., Cesa, S. (2016). Evaluation of
515 different extraction methods from pomegranate whole fruit or peels and the antioxidant and
516 antiproliferative activity of the polyphenolic fraction. *Food Chemistry*, 202, 59–69.

517 Mosquera, M., Giménez, B., Mallmann da Silva, I., Ferreira Boelter, J., Montero, P., Gómez-
518 Guillén, M.C., Brandelli, A. (2014). Nanoencapsulation of an active peptidic fraction from sea
519 bream scales collagen. *Food Chemistry*, 156, 144–150.

520 Mozafari, M.R., Johnson, C., Hatziantoniou, S. and Demetzos, C. (2008). Nanoliposomes and
521 their applications in food nanotechnology. Journal of Liposome Research, 18 (4), 309–327.

522 Müller, R.H., Jacobs, C., Kayser, O. (2001). Nanosuspensions as particulate drug formulations in
523 therapy: rationale for development and what we can expect for the future. *Advanced Drug*
524 *Delivery Reviews*, 47 (1), 3–19.

525 Neunert, G., Górnaś, P., Dwiecki, K., Siger, A., Polewski, K. (2015). Synergistic and antagonistic
526 effects between alpha-tocopherol and phenolic acids in liposome system: spectroscopic study.
527 *European Food Research and Technology*, 241, 749–757.

528 Pawlikowska-Pawlęga, B., Dziubińska, H., Król, E., Trębacz, K., Jarosz-Wilkołazka, A., Paduch, R.,
529 Gawron, A., Gruszecki, W.I. (2014). Characteristics of quercetin interactions with liposomal and
530 vacuolar membranes. *Biochimica et Biophysica Acta - Biomembranes*, 1838 (1, PARTB), 254–
531 265.

532 Popova, A.V., Hincha, D.K. (2016). Effects of flavonol glycosides on liposome stability during
533 freezing and drying. *Biochimica et Biophysica Acta - Biomembranes*, 1858, 3050–3060.

534 Pamplona, R. (2008). Membrane phospholipids, lipoxidative damage and molecular integrity: A
535 causal role in aging and longevity. Biochimica et Biophysica Acta (BBA) – Bioenergetics, 1777,
536 1249-126.

537 Ramdath, D.D., Padhi, E.M.T., Sarfaraz, S., Renwick, S., Duncan, A.M. (2017). Beyond the
538 cholesterol-lowering effect of soy protein: a review of the effects of dietary soy and its
539 constituents on risk factors for cardiovascular disease. *Nutrients*, 9 (4), 324.

540 Ramezanzade, L., Hosseini, S.F., Nikkhah, M. (2017). Biopolymer-coated nanoliposomes as
541 carriers of rainbow trout skin-derived antioxidant peptides. *Food Chemistry*, 234, 220–229.

542 Semenova, M.G., Antipova, A.S., Zelikina, D.V., Martirosova, E.I., Plashchina, I.G., Palmina, N.P.,
543 Binyukov, V.I., Bogdanova, N.G., Kasparov, V.V., Shumilina, E.A., Ozerova, N.S. (2016).
544 Biopolymer nanovehicles for essential polyunsaturated fatty acids: Structure–functionality
545 relationships. *Food Research International*, 88, 70–78.

546 Sharma, A., Sharma, U.S. (1997). Liposomes in drug delivery: Progress and limitations.
547 International Journal of Pharmaceutics, 154, 123–140.

548 Singh, H. (2016). Nanotechnology applications in functional foods; Opportunities and
549 challenges. *Preventive Nutrition and Food Science*, 21, 1–8.

550 Stark, B., Pabst, G., Prassl, R. (2010). Long-term stability of sterically stabilized liposomes by
551 freezing and freeze-drying: Effects of cryoprotectants on structure. *European Journal of*
552 *Pharmaceutical Sciences*, 41 (3–4), 546–555.

553 Sułkowski, W.W., Pentak, D., Nowak, K., Sułkowska, A. (2005). The influence of temperature,
554 cholesterol content and pH on liposome stability. *Journal of Molecular Structure*, 744–747,
555 737–747.

556 Taladrid, D., Marín, D., Alemán, A., Álvarez-Acero, I., Montero, P., Gómez-Guillén, M.C. (2017).
557 Effect of chemical composition and sonication procedure on properties of food-grade soy
558 lecithin liposomes with added glycerol. *Food Research International*, 100, 541–550.

559 Tan, C., Xia, S., Xue, J., Xie, J., Feng, B., Zhang, X. (2013). Liposomes as vehicles for lutein:
560 Preparation, stability, liposomal membrane dynamics, and structure. *Journal of Agricultural*
561 *and Food Chemistry*, 61, 8175–8184.

562 Toyran, N., Severcan, F. (2003). Competitive effect of vitamin D_2 and Ca^{2+} on phospholipid
563 model membranes: An FTIR study. *Chemistry and Physics of Lipids*, 123 (2), 165–176.

564 Wang, G., Wang, T. (2008). Oxidative Stability of Egg and Soy Lecithin as Affected by Transition
565 Metal Ions and pH in Emulsion. *Journal of Agricultural and Food Chemistry*, 56, 11424–11431.

566 Ye, T., Yu, J., Luo, Q., Wang, S., Chan, H.K. (2017). Inhalable clarithromycin liposomal dry
567 powders using ultrasonic spray freeze drying. *Powder Technology*, 305, 63–70.

568

FIGURE CAPTIONS

FIGURE 1. Cryo-TEM images of fresh liposomes: (a) L-E: empty liposomes; (b) L-HC: liposomes with collagen hydrolysate; (c) L-PG: liposomes with pomegranate extract; (d) L-SL: liposomes with shrimp lipid extract.

FIGURE 2. Cryo-TEM images of newly freeze-dried liposomal pastes: (a) L-HC: liposomes with collagen hydrolysate; (b) L-PG: liposomes with pomegranate extract; (c) L-SL: liposomes with shrimp lipid extract.

FIGURE 3. DSC traces of: (a) fresh liposomal suspensions; (b) newly freeze-dried liposomal pastes.
L-HC: liposomes with collagen hydrolysate; L-PG: liposomes with pomegranate extract; L-SL: liposomes with shrimp lipid extract.

FIGURE 4. Frequency variations in stretching modes of selected functional groups determined in freeze-dried liposomal pastes: (a) CH_2 asymmetric stretching vibration; (b) C=O stretching vibration; (c) PO_2^- antisymmetric double bond stretching vibration.
L-HC: liposomes with collagen hydrolysate; L-PG: liposomes with pomegranate extract; L-SL: liposomes with shrimp lipid extract.

FIGURE 5. Mechanical spectra of newly freeze-dried liposomal pastes: (a) Elastic modulus (G', Pa); (b) Viscous modulus (G", Pa).
L-HC: liposomes with collagen hydrolysate; L-PG: liposomes with pomegranate extract; L-SL: liposomes with shrimp lipid extract.

FIGURE 6. Viscoelastic parameters, determined at 1 Hz, of the newly freeze-dried liposomal pastes and pastes stored for 7 months: (a) Elastic modulus (G', Pa); (b) Viscous modulus (G", Pa); (c) phase angle (δ, °); (d) power law exponent (n').
L-HC: liposomes with collagen hydrolysate; L-PG: liposomes with pomegranate extract; L-SL: liposomes with shrimp lipid extract.

FIGURE 7. Viscoelastic properties as a function of temperature of the newly freeze-dried liposomal pastes: (a) Elastic modulus (G', Pa), (b) Viscous modulus (G", Pa); and pastes stored for 7 months: (c) Elastic modulus (G', Pa), (d) Viscous modulus (G", Pa).
L-HC: liposomes with collagen hydrolysate; L-PG: liposomes with pomegranate extract; L-SL: liposomes with shrimp lipid extract.

606

607

608 Table 1. Particle size (expressed as z-average), polydispersity index (PDI) and zeta potential of fresh liposomes
609 stored for 2 weeks at 4 °C and freeze-dried liposomes stored for 7 months at –20 °C.

		Fresh			Freeze-dried		
		0 weeks	1 weeks	2 weeks	0 months	3 months	7 months
z-average (nm)	L-E	$87.4\pm0.8^{B/M}$	$85.7\pm0.0^{A/M}$	$86.2\pm0.9^{A,B/M}$	$316.6\pm6.7^{c/N}$	$261.0\pm3.5^{b/P}$	$159.0\pm2.7^{a/M}$
	L-HC	$102.3\pm0.8^{A/N}$	$104.2\pm1.1^{B/N}$	$104.7\pm0.4^{B/N}$	$274.9\pm5.5^{b/M}$	$183.3\pm2.0^{a/O}$	$177.4\pm2.6^{a/N}$
	L-PG	$104.2\pm0.8^{A/N}$	$104.0\pm0.9^{A/N}$	$105.5\pm0.8^{A/N}$	$256.8\pm2.3^{b/M}$	$174.5\pm3.6^{a/N}$	$178.2\pm2.3^{a/N}$
	L-SL	$102.2\pm1.6^{A/N}$	$105.0\pm0.8^{A,B/N}$	$107.0\pm1.7^{B/N}$	$372.9\pm15.9^{b/O}$	$150.0\pm0.6^{a/M}$	$159.2\pm2.4^{a/M}$
PDI	L-E	$0.240\pm0.005^{A/M}$	$0.241\pm0.007^{A/M}$	$0.230\pm0.007^{A/M}$	$0.374\pm0.081^{a/M}$	$0.316\pm0.035^{a/N}$	$0.368\pm0.018^{a/N}$
	L-HC	$0.247\pm0.019^{A/M}$	$0.256\pm0.007^{A/M}$	$0.256\pm0.006^{A/M,N}$	$0.334\pm0.033^{a,b/M}$	$0.386\pm0.012^{b/O}$	$0.311\pm0.033^{a/M}$
	L-PG	$0.263\pm0.017^{A/M}$	$0.263\pm0.008^{A/M}$	$0.264\pm0.016^{A/N}$	$0.279\pm0.021^{a/M}$	$0.319\pm0.021^{a/N}$	$0.293\pm0.026^{a/M}$
	L-SL	$0.246\pm0.017^{A/M}$	$0.254\pm0.015^{A/M}$	$0.264\pm0.015^{A/N}$	$0.408\pm0.112^{a/M}$	$0.264\pm0.009^{a/M}$	$0.258\pm0.005^{a/M}$
Zeta potential (mV)	L-E	$-35.5\pm1.7^{B/N}$	$-38.9\pm1.1^{A,B/M}$	$-43.7\pm3.7^{A/M}$	$-54.2\pm1.5^{a/N}$	$-47.8\pm1.2^{b/M,N}$	$-45.5\pm1.0^{b/M}$
	L-HC	$-43.4\pm0.7^{A/M}$	$-41.5\pm1.7^{A/M}$	$-31.7\pm0.6^{B/O}$	$-54.9\pm0.7^{a/N}$	$-50.8\pm1.8^{b/M}$	$-49.8\pm1.2^{b/N}$
	L-PG	$-38.2\pm0.7^{A/N}$	$-40.4\pm1.8^{A/M}$	$-38.8\pm0.7^{A/N}$	$-57.2\pm0.5^{a/M,N}$	$-45.2\pm2.1^{b/N}$	$-46.6\pm2.1^{b/M,N}$
	L-SL	$-41.9\pm2.2^{A/M}$	$-41.2\pm0.8^{A/M}$	$-32.9\pm0.7^{B/O}$	$-59.1\pm2.2^{a/M}$	$-44.1\pm1.1^{b/N}$	$-47.5\pm1.8^{b/M,N}$

610 L-E: empty liposomes; L-HC: liposomes with collagen hydrolysate; L-PG: liposomes with pomegranate extract; L-SL: liposomes with shrimp
611 lipid extract. Different letters (A, B) indicate significant differences ($p\leq0.05$) in fresh liposomes as a function of time. Different letters (a, b,
612 c) indicate significant differences ($p\leq0.05$) in freeze-dried liposomes as a function of time. Different letters (M, N, O, P) indicate significant
613 differences ($p\leq0.05$) among liposome formulations.

614

615

616

617 Table 2. Moisture content, water solubility and thiobarbituric acid reactive substances (TBARS)
618 of newly fresh liposomes and freeze-dried liposomes stored for 7 months at –20 °C.

		Fresh	Freeze-dried		
		0 weeks	0 months	3 months	7 months
Moisture (%)	L-E	91.97 ± 0.57^{M}	$18.48 \pm 2.20^{a/M}$	$16.60 \pm 2.38^{a/N}$	$17.06 \pm 1.33^{a/M}$
	L-HC	92.75 ± 0.27^{M}	$21.30 \pm 1.10^{b/M}$	$10.03 \pm 2.30^{a/M}$	$11.74 \pm 2.29^{a/M}$
	L-PG	92.65 ± 0.36^{M}	$24.39 \pm 2.64^{b/M}$	$10.27 \pm 2.36^{a/M}$	$15.12 \pm 4.33^{a/M}$
	L-SL	92.77 ± 0.50^{M}	$24.87 \pm 4.55^{b/M}$	$10.09 \pm 1.78^{a/M}$	$18.62 \pm 4.11^{b/M}$
Solubility (%)	L-E	74.34 ± 11.49^{M}	$73.63 \pm 2.62^{a/N}$	$73.54 \pm 0.69^{a/N}$	$73.56 \pm 1.77^{a/N}$
	L-HC	87.36 ± 3.98^{M}	$76.45 \pm 0.37^{a/N}$	$74.51 \pm 1.53^{a/N}$	$87.12 \pm 2.50^{b/N}$
	L-PG	83.90 ± 3.93^{M}	$80.90 \pm 1.66^{a/O}$	$78.64 \pm 3.59^{a/N}$	$85.25 \pm 13.17^{a/N}$
	L-SL	87.60 ± 3.99^{M}	$65.22 \pm 1.33^{b/M}$	$49.69 \pm 4.19^{a/M}$	$56.24 \pm 5.77^{a,b/M}$
TBARS (µg MDA eq/kg dry matter)	L-E	8.22 ± 1.94^{M}	$81.8 \pm 3.56^{M/a}$	$65.2 \pm 1.29^{M/b}$	$38.5 \pm 0.70^{M/c}$
	L-HC	18.4 ± 2.10^{O}	$69.2 \pm 2.97^{N/a}$	$44.2 \pm 1.25^{N/b}$	$32.3 \pm 1.30^{N/c}$
	L-PG	9.80 ± 0.00^{MN}	$46.6 \pm 2.86^{P/a}$	$24.7 \pm 5.89^{P/b}$	$23.5 \pm 1.23^{O/b}$
	L-SL	12.4 ± 1.05^{N}	$58.5 \pm 4.74^{O/a}$	$33.3 \pm 4.31^{O/b}$	$15.5 \pm 0.29^{P/c}$

619 L-E: empty liposomes; L-HC: liposomes with collagen hydrolysate; L-PG: liposomes with pomegranate
620 extract; L-SL: liposomes with shrimp lipid extract. Different letters (M, N, O, P) indicate significant
621 differences ($p \leq 0.05$) among liposome formulations. Different letters (a, b, c) indicate significant differences
622 ($p \leq 0.05$) in freeze-dried liposomes as a function of time.

623

Table 3. Entrapment efficiency of freeze-dried liposomes stored for 7 months at –20 °C.

	Entrapment efficiency (%)		
	0 months	3 months	7 months
L-HC	$87.25 \pm 1.97^{a/M}$	$86.61 \pm 5.08^{a/M}$	$89.60 \pm 2.20^{a/M}$
L-PG	$63.19 \pm 3.90^{a/N}$	$62.88 \pm 1.71^{a/N}$	$62.44 \pm 3.03^{a/N}$
L-SL	$97.24 \pm 0.08^{a/M}$	$96.92 \pm 0.00^{a/M}$	$96.96 \pm 0.09^{a/M}$

L-HC: liposomes with collagen hydrolysate; L-PG: liposomes with pomegranate extract; L-SL: liposomes with shrimp lipid extract. Different letters (M, N, O, P) indicate significant differences ($p \leq 0.05$) among liposome formulations. Different letters (a, b, c) indicate significant differences ($p \leq 0.05$) as a function of time.

634

635

636 Table 4. Colour parameters of newly freeze-dried liposomes

	Colour parameters				
	L*(D65)	a*(D65)	b*(D65)	Chroma	Hue angle (°)
L-E	32.52 ± 0.22^{A}	0.95 ± 0.09^{A}	8.27 ± 0.14^{A}	8.32 ± 0.15^{A}	83.46 ± 0.53^{A}
L-HC	32.71 ± 0.22^{A}	3.23 ± 0.20^{B}	10.54 ± 0.18^{B}	11.02 ± 0.22^{B}	72.99 ± 0.80^{B}
L-PG	27.81 ± 0.22^{B}	2.33 ± 0.07^{C}	5.27 ± 0.27^{C}	5.76 ± 0.27^{C}	66.12 ± 0.79^{C}
L-SL	29.06 ± 0.25^{C}	7.10 ± 0.21^{D}	5.80 ± 0.22^{D}	9.17 ± 0.30^{D}	39.25 ± 0.45^{D}

637 L-HC: liposomes with collagen hydrolysate; L-PG: liposomes loaded pomegranate extract; L-SL:
638 liposomes with shrimp lipid extract. Different letters (A, B, C, …) indicate significant differences ($p \leq 0.05$)
639 among liposome formulations.
640

641
642

643 Table 5. Transition temperatures and enthalpy
644 changes in fresh and freeze-dried liposomes
645 stored for 7 months at –20 °C.

	$T_{peak\ 1}$ (°C)	Enthalpy (J/g)
Fresh		
L-E	-6.59±0.20^{a}	120.6±0.64^{a}
L-HC	-3.91±0.40^{bc}	171.6±0.07^{bcd}
L-PG	-4.24±0.66^{b}	161.8±4.38^{b}
L-SL	-4.29±0.35^{b}	166.8±3.81^{bc}
Dry – 0 months		
L-E	3.98±1.06^{a}	-
L-HC	2.04±0.50^{b}	-
L-PG	1.76±0.47^{b}	-
L- SL	11.05±0.93^{c}	-
Dry – 3 months		
L-E	0.85±0.86^{bd}	-
L-HC	1.15±0.92^{b}	-
L-PG	0.88±0.08^{b}	-
L- SL	9.69±0.38^{c}	-
Dry – 7 months		
L-E	-0.53±0.27^{de}	-
L-HC	-1.30±0.48^{e}	-
L-PG	1.66±0.00^{b}	-
L- SL	10.19±0.13^{c}	-

646 L-E: empty liposomes; L-HC: liposomes with collagen
647 hydrolysate; L-PG: liposomes with pomegranate extract; L-SL:
648 liposomes with shrimp lipid extract. Different letters (a, b, c,
649 …) indicate significant differences ($p \leq 0.05$) as a function of
650 liposome formulation and time.

651

652

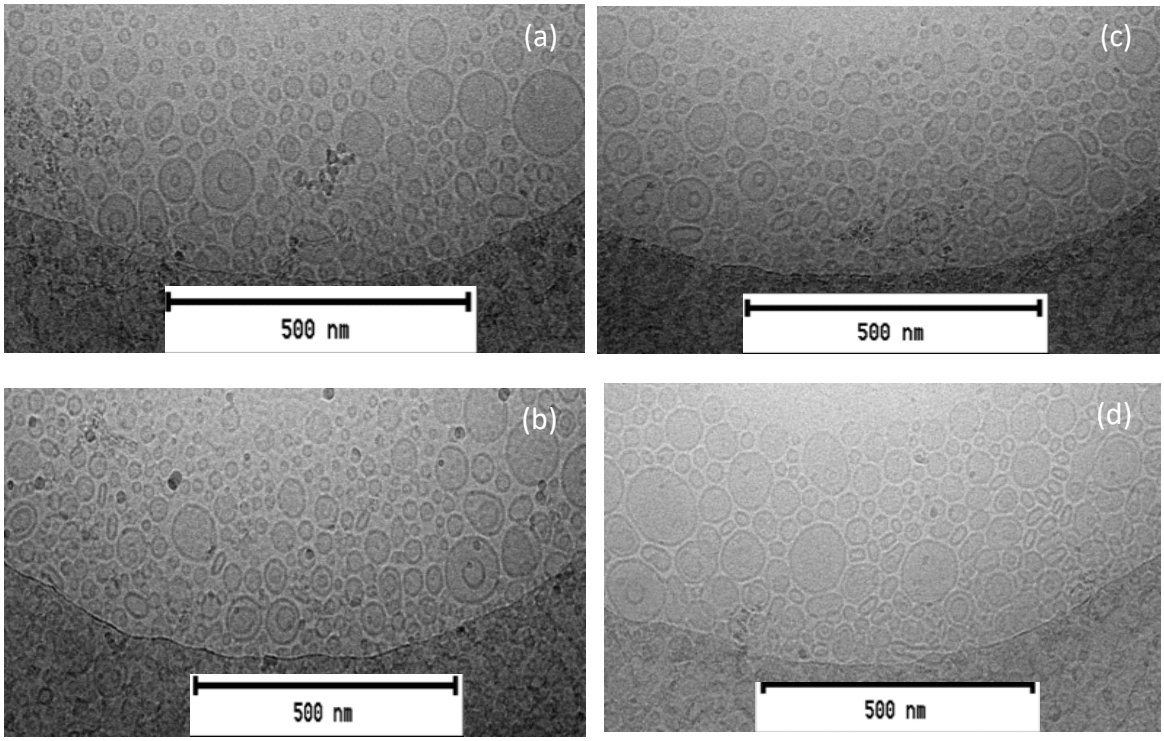

FIGURE 1. Cryo-TEM images of fresh liposomes: (a) L-E: empty liposomes;
(b) L-HC: liposomes with collagen hydrolysate; (c) L-PG: liposomes with pomegranate extract;
(d) L-SL: liposomes with shrimp lipid extract

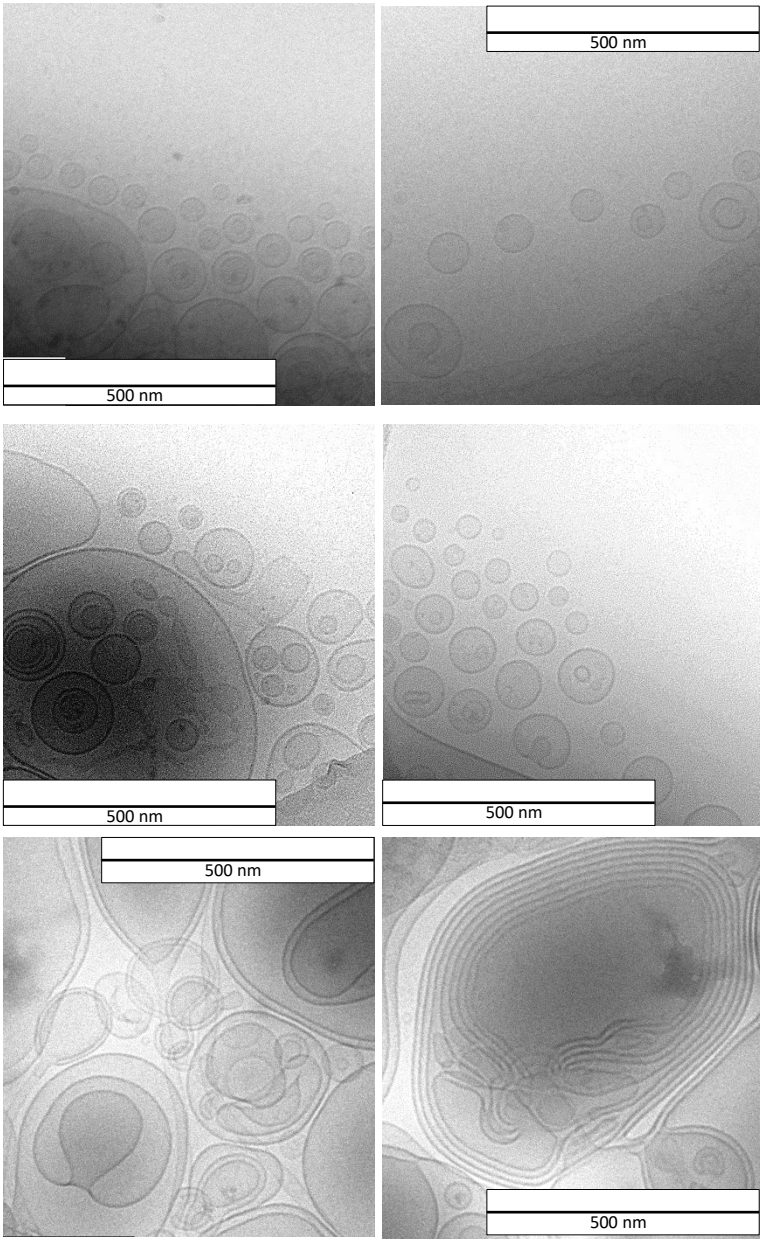

FIGURE 2. Cryo-TEM images of newly freeze-dried liposomal pastes:
(a) L-HC: liposomes with collagen hydrolysate; (b) L-PG: liposomes with
(b) pomegranate extract; (c) L-SL: liposomes with shrimp lipid extract.

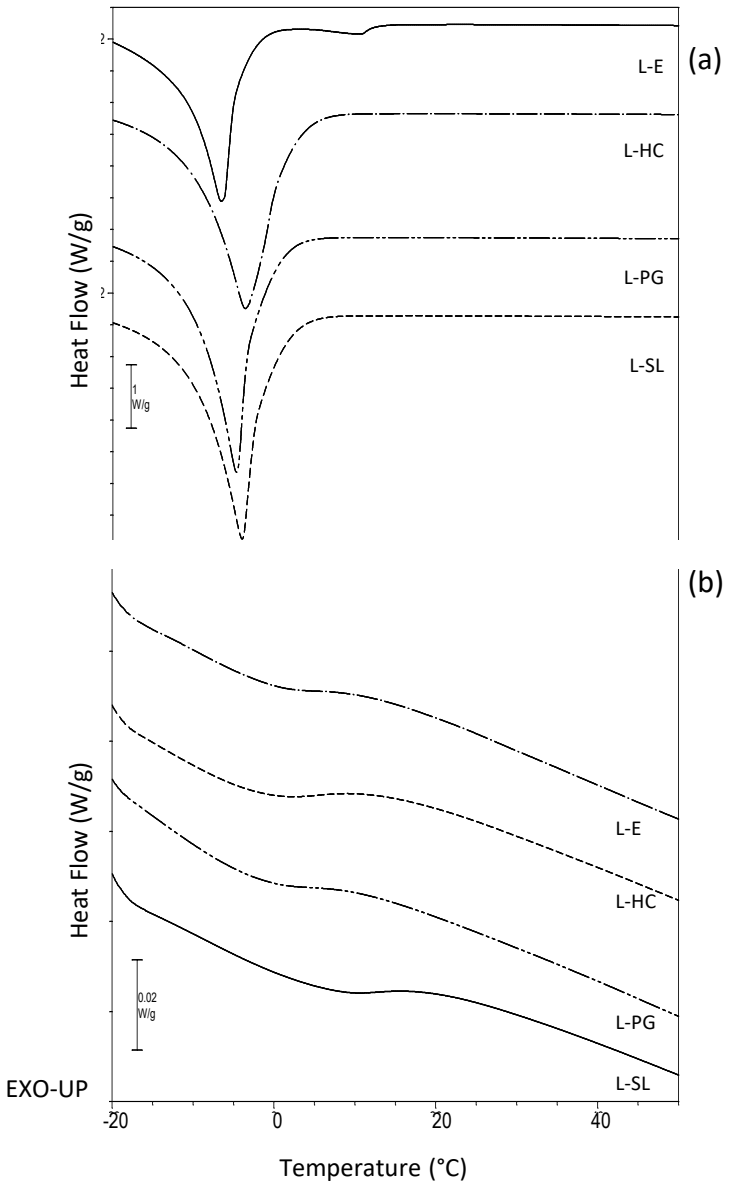

FIGURE 3. DSC traces of: (a) fresh liposomal suspensions;
(b) newly freeze-dried liposomal pastes.
L-HC: liposomes with collagen hydrolysate; L-PG: liposomes
with pomegranate extract; L-SL: liposomes with shrimp lipid extract.

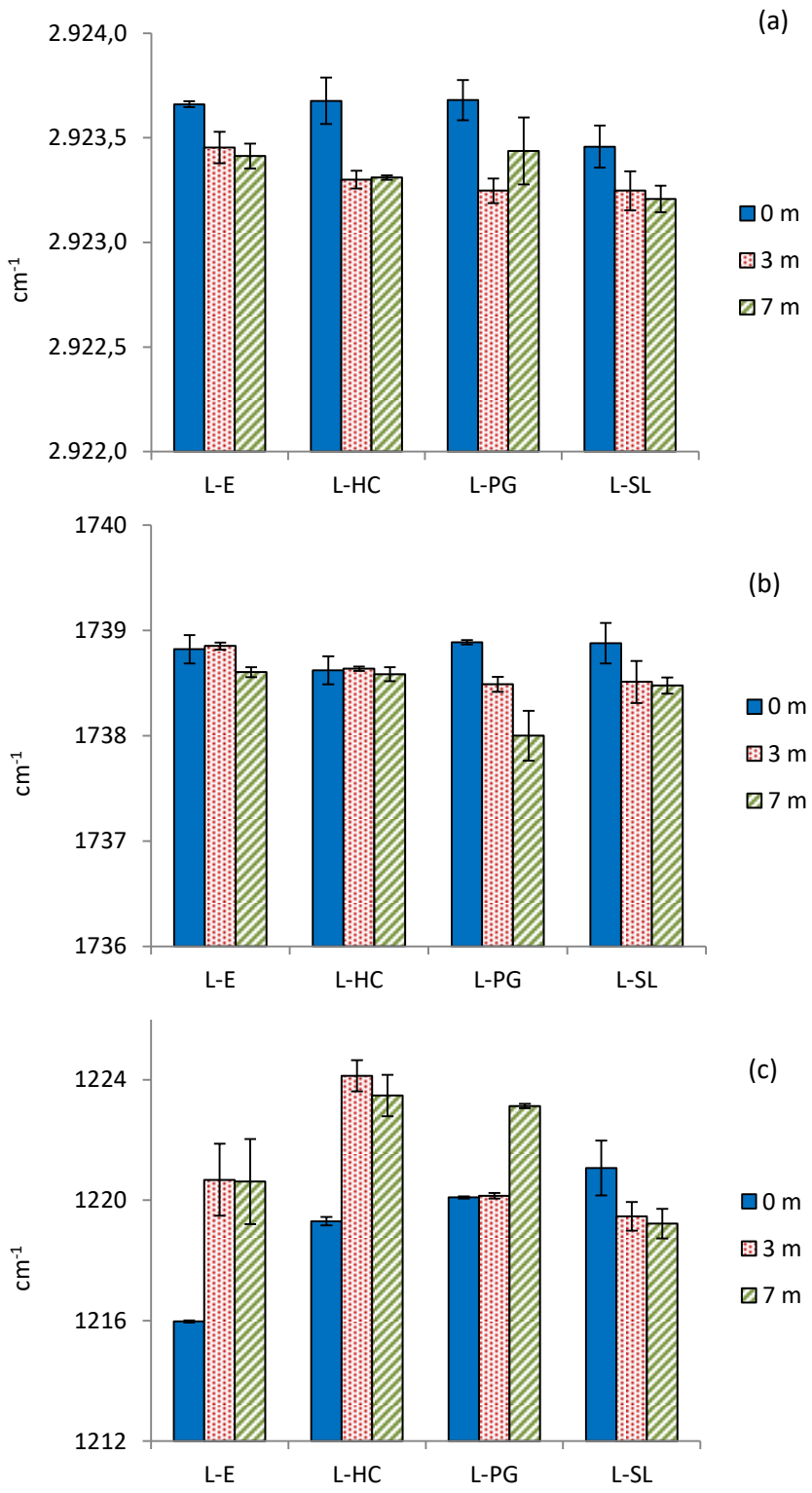

FIGURE 4. Frequency variations in stretching modes of selected functional groups determined in freeze-dried liposomal pastes: (a) CH2 asymmetric stretching vibration; (b) C=O stretching vibration; (c) PO2- antisymmetric double bond stretching vibration. L-HC: liposomes with collagen hydrolysate; L-PG: liposomes with pomegranate extract; L-SL: liposomes with shrimp lipid extract.

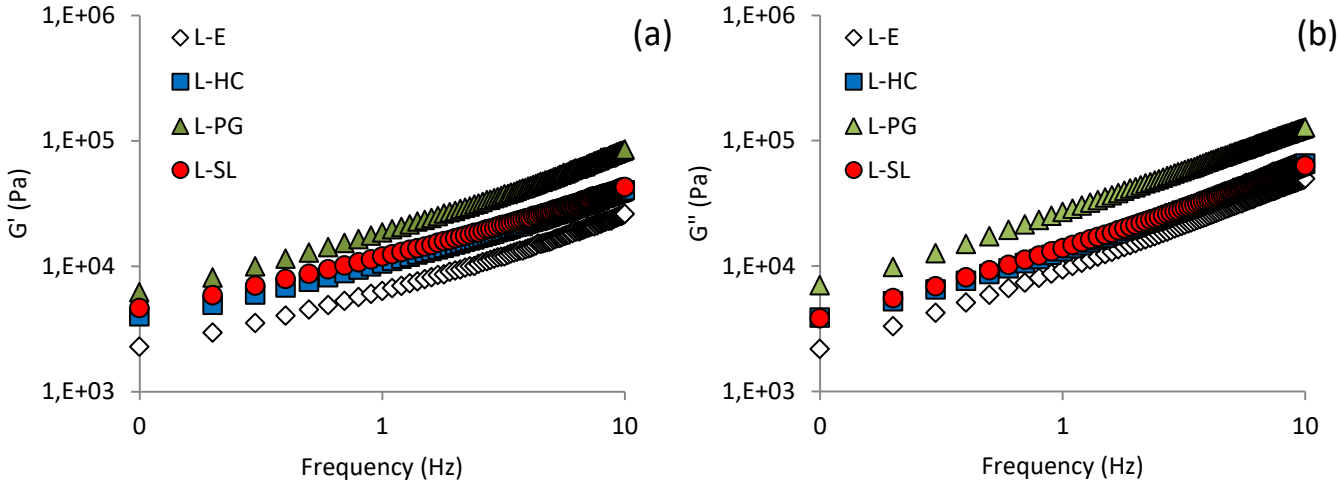

FIGURE 5. Mechanical spectra of newly freeze-dried liposomal pastes: (a) Elastic modulus (G', Pa); (b) Viscous modulus (G", Pa).
L-HC: liposomes with collagen hydrolysate; L-PG: liposomes with pomegranate extract; L-SL: liposomes with shrimp lipid extract

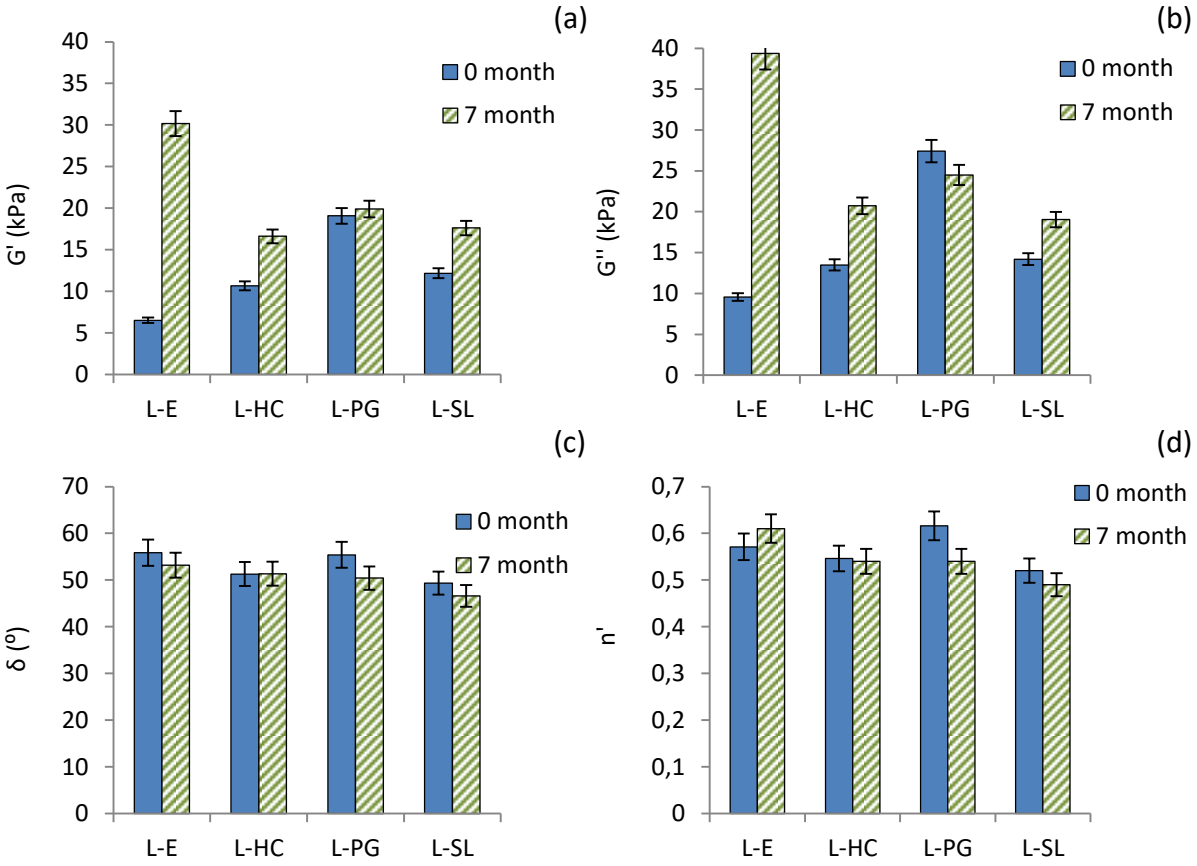

FIGURE 6. Viscoelastic parameters, determined at 1 Hz, of the newly freeze-dried liposomal pastes and pastes stored for 7 months: (a) Elastic modulus (G′, Pa); (b) Viscous modulus (G″, Pa); (c) phase angle (δ, °); (d) power law exponent (n′).
L-HC: liposomes with collagen hydrolysate; L-PG: liposomes with pomegranate extract; L-SL: liposomes with shrimp lipid extract.

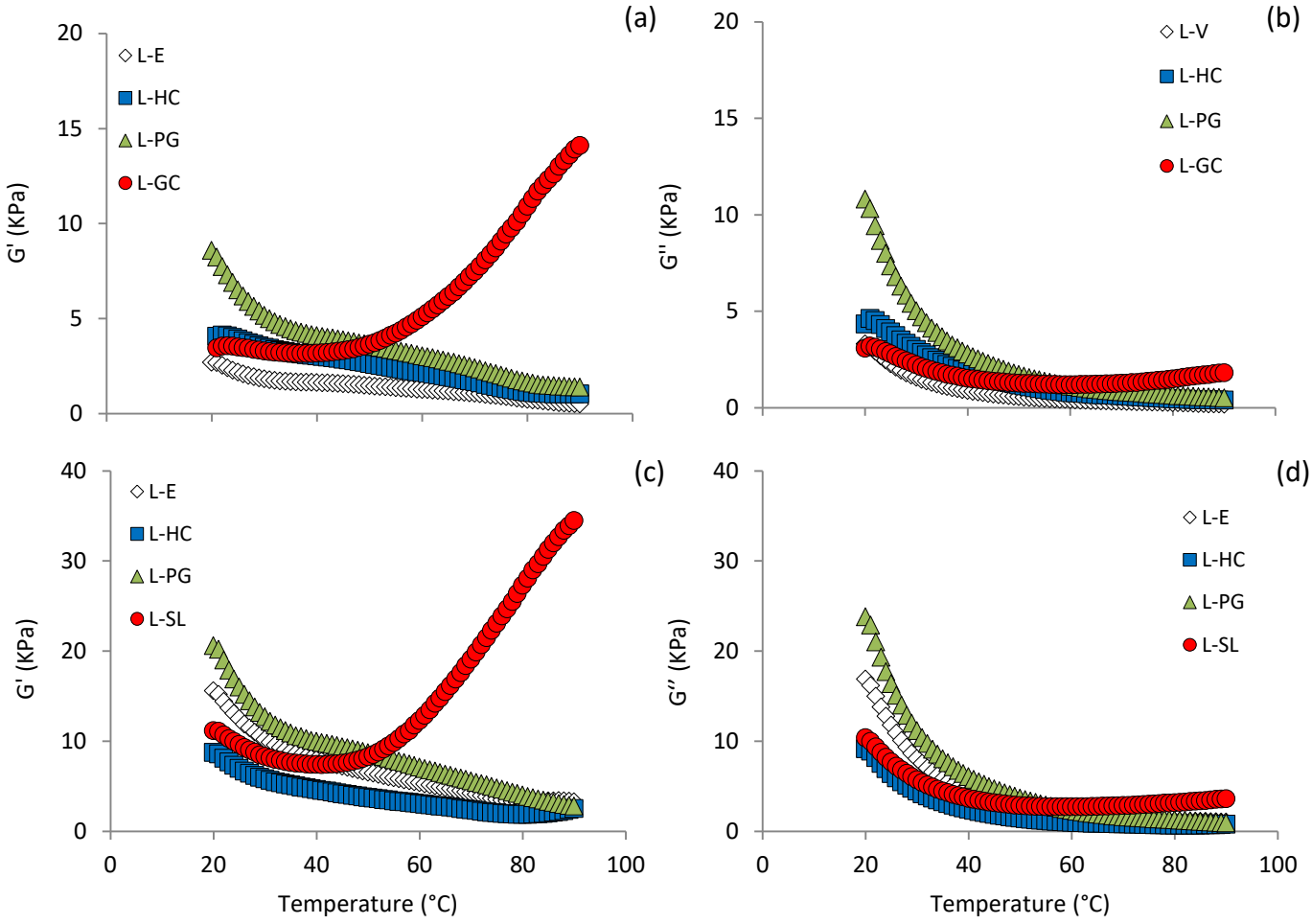

FIGURE 7. Viscoelastic properties as a function of temperature of the newly freeze-dried liposomal pastes : (a) Elastic modulus (G', Pa), (b) Viscous modulus (G", Pa); and pastes stored for 7 months: (c) Elastic modulus (G', Pa), (d) Viscous modulus (G", Pa).
L-HC: liposomes with collagen hydrolysate; L-PG: liposomes with pomegranate extract; L-SL: liposomes with shrimp lipid extract.

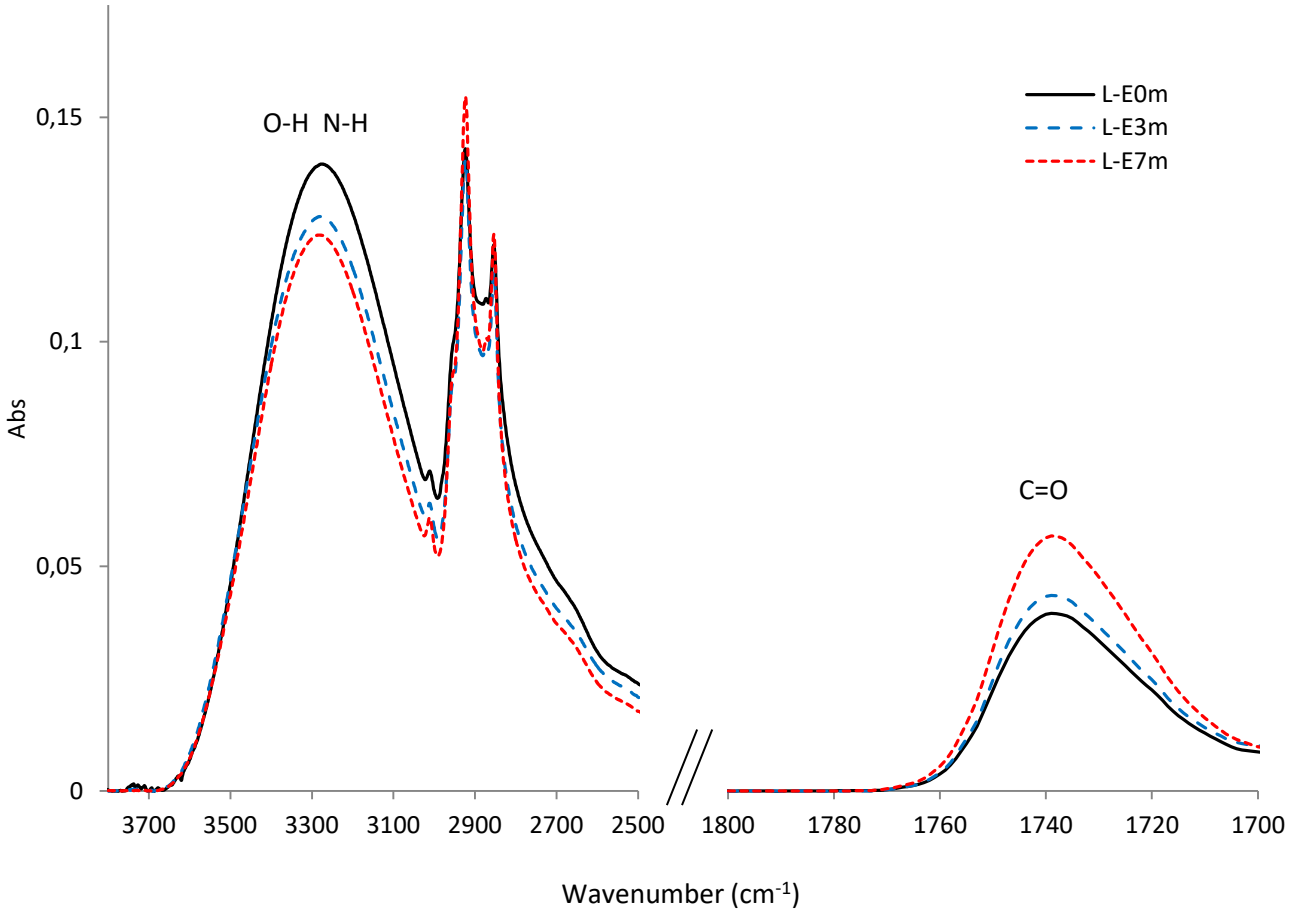

FIGURE 8. Infrared spectroscopy (ATR-FTIR) changes associated to lipid oxidation in freeze-dried empty liposomes (L-E) during seven months of frozen storage .